

Grey-Taguchi Approach to Optimize Fused Deposition Modeling Process in Terms of Mechanical Properties and Dimensional Accuracy

Md Asif Bin Syed¹, Qausar Rhaman², Hasan Md. Shahriar², and Mohammad Mushshin Aziz Khan²

¹Industrial and Management Systems Engineering, West Virginia University, United States

²Department of Industrial and production Engineering, Shahjalal University of Science and Technology, Sylhet 3114, Bangladesh,

Email: ms00110@mix.wvu.edu*, qrhaman@gmail.com, hasanmd.shahriar@yahoo.com, muhshin-ipe@sust.edu,

*Corresponding Author [Md Asif Bin Syed]

- 3D Printing;
- Rapid Prototyping;
- Grey-Taguchi Approach;
- Fused Deposition Modeling;
- Parametric Effects;
- Optimization;
- Additive Manufacturing.

Abstract: Fused Deposition Modeling (FDM) is a process that allows for the rapid production of functional parts through the deposition of fused material layers in a sequential manner. FDM has flexibility and the potential to create complicated parts. This study aims to optimize the FDM process parameters in terms of tensile strength, flexural strength, and longitudinal shrinkage using the Grey-Taguchi approach. The input parameters chosen to study the effects on dimension and mechanical properties are layer thickness, the raster angle, fill density, the number of contours, printing temperature, and printing speed. The Taguchi L27 orthogonal array is used as the statistical design of experiment (DOE) technique to assess how the FDM process behaves with the change in process input parameters selected. The ANOVA test was used to assess the contribution and implications of each response factor of the FDM process on the FDM process. Additionally, the optimization of multiple characteristics is done by Grey relational analysis. Optimal parameter settings that minimize longitudinal shrinkage and maximize tensile and flexural strengths concurrently are 0.2 mm of layer thickness, 90-degree raster angle, fill density of 30, 16 numbers of contours, 230°C printing temperature, and a printing speed of 60 mm/s.

1 Introduction

Rapid prototyping (RP) is a concept that is used in a wide range of industries to depict a process for producing a model of the system or part prior to full version or commercialization [1]. Additive Manufacturing (AM) is

the standardized term for what was previously referred to as rapid prototyping, and what is often referred to as 3D printing, both of which are technologies that are becoming increasingly popular. According to ASTM, “AM can be defined as a collection of technologies able to join materials to make objects from 3D model

data, usually layer upon layer, as opposed to subtractive manufacturing methodologies” [2]. Several types of additive manufacturing processes are Vat Photopolymerization, Powder Bed Fusion, Binder Jetting (3D printing), Material Jetting, Sheet Lamination, Material Extrusion, directed energy deposition, and so on [3]. Fused Deposition Modeling (FDM) is widely used extrusion-based additive manufacturing techniques which is developed by Stratasys, a United States- based organization. Polymer filaments are introduced into the FDM system through a heating chamber, which liquefies the polymer. The filament is then driven into the extrusion chamber using tractor wheels, which creates the extrusion pressure in the chamber [4]. Other popularly used 3D printing techniques are- Stereolithography (SLA), Digital Light Processing (DLP), Selective Laser Sintering (SLS), Selective Laser Melting (SLM), Laminated Object Manufacturing (LOM), Digital Beam Melting (EBM).

A considerable amount of literature has been published on process parameter optimization of the 3D printing process. These studies have shown the influence of various 3D printing parameters over tensile strength, flexural strength, and longitudinal shrinkage. A study from Lung Kwang Pan [5] showed that three 3D-printing processing parameters such as extrusion temperature, printing speed, and layer height with proper processing control can make parts as strong as injection-molded counterparts. According to experimental results by Vaezi [6], considering the layer thickness as constant an increase in the binder saturation level from 90% to 125% will result in high tensile and flexural strength. However, the dimensional accuracy and surface uniformity will be decreased. On the other hand, an increase in layer thickness from 0.087 to 0.1 mm would result in a drop in tensile strength and an increase in flexural strength under the same conditions of binder saturation. Lanzotti et al. [7] found the relation among the infill orientation, layer thickness and the number of layers or perimeter and their combined effect on mechanical strength. In particular, the strength increases as the infill orientation decreases with a rate which is as higher as the layer thickness increases. Similar results are observed considering the combined effects of the infill orientation and the number of perimeters. Samir Kumar Panda et al. [8] demonstrated the effect of input variables (air gap, raster

angle, orientation, raster width, and layer thickness) on tensile and flexural strength. According to Said et al. [9], the raster orientation aligns polymer molecules with the direction of deposition during manufacturing of a component with increased tensile, flexural, and impact strength depending on the orientation of the sample. Another group of researchers examined the process parameters of FDM such as raster orientation, air gap, bead width, color, and model temperature using the design of experiments (DOE) [10]. Considering several essential parameters, they together can have a significant effect on the 3D printing process. However, there are very few studies that are performed by combining a wide variety of input parameters. So, this study took a unique combination of six input parameters of FDM, e.g., layer thickness, raster angle, printing speed, temperature, fill density, and the number of contours. Studying the combined effects of those parameters of 3D Printing are the novelty of this research.

According to the literature review, numerous optimization techniques were used to optimize FDM process parameters, including grey relational, full factorial, taguchi method, response surface methodology (RSM), fractional factorial, genetic algorithm, fuzzy logic, and artificial neural network (ANN). The Grey Taguchi method and the ANOVA technique are the most often used optimization approaches [11]. It is highlighted that compared to RSM; the Taguchi approach can significantly minimize the number of tests. Grey-Taguchi is utilized instead of Taguchi because Taguchi produces superior output responses when there is only one output feature. However, Grey-Taguchi can display the relationship between many output characteristics. Another technique is the full factorial design, enabling the researcher to investigate the impact of process input factors on response outputs. For process parameters, the primary impacts and all higher-order interactions can be approximated. The primary disadvantage of a full factorial design is that it requires more experiments to attain higher precision and a lower percentage of error [12]. As a result, most experiments, especially those involving advanced manufacturing technologies like FDM, are time-consuming and costly. Because of these considerations, researchers favor fractional factorial design over full factorial design, which requires fewer runs. Thus, the primary motivation

for employing the Grey-Taguchi approach is to obtain a higher-order response with fewer necessary runs than is possible with a traditional factorial design. This strategy is appropriate for our study as each of its input variables requires three levels. Grey-Taguchi optimization – a type of Design of Experiment (DOE) – was used in this study to optimize the process by generating higher-order responses with fewer trials. Thus, this study employs the Grey-Taguchi approach to optimize the process parameters of the fused deposition model.

2 Experimental Procedure

2.1 Materials

In this work, the FDM method is demonstrated using carbon fiber PLA. Carbon fiber PLA filaments are made by infusing tiny carbon fibers into the PLA base material to enhance their strength and stiffness further. Aliphatic thermoplastic polyester made from renewable resources. PLA was the second most consumed bioplastic on a global scale in 2010, despite it still not being a commodity polymer. Perhaps the primary advantage of PLA is its reduced shrinkage and lower melting point. The former lessens residual stresses in the printed items, eliminating deformation and delamination, while the latter increases the printing process's productivity.

2.2 Design of the Specimen

2.2.1 Tensile Test Specimen Design

The specimen was designed following the dimensions specified in ASTM D638-14 (Type I) for the tensile test, as shown in Table 1. Solidworks 3D Modelling software was used to design the specimen for the tensile test which is shown in Figure 1. The design was saved in an STL format for 3D printing.

2.2.2 Flexural Test Specimen Design

As shown in Table 2, the specimen was designed for the flexural strength test following the dimensions specified in ASTM D790-03. In this study, the specimen (Fig 2) was designed using Solidworks 3D Modelling Software and saved in an STL format for 3D printing.

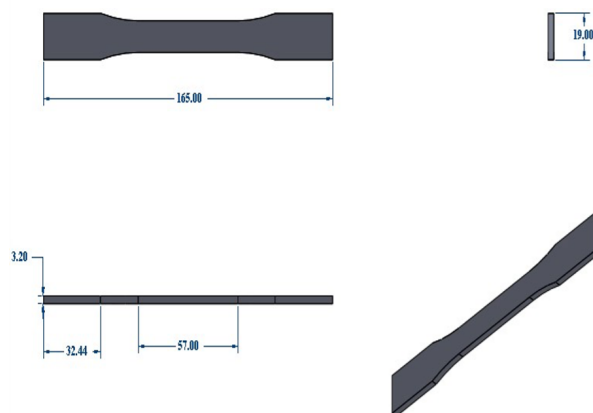


Figure 1: Tensile test specimen dimensions.

Table 1: Tensile test specimen dimensions.

Dimensions	Measurement in mm
W-Width of narrow section	13
L-Length of narrow section	57
Wo-Width overall	19
I-Length overall	165
G-Gage length	50
d-Distance between grips	115
r-Radius of fillet	76
T-Thickness	3.2

2.2.3 Longitudinal Shrinkage

Shrinkage can be a severe concern when printing 3D items. ABS and PLA are the most frequently used plastics for personal 3D printing. ABS is stronger and somewhat more flexible than PLA, which is biodegradable and available in a wider variety of vibrant colors. For the shrinkage test, both the tensile and flexural test specimens were used. After printing the specimen, they were measured using Vernier slider calipers with a resolution of 0.02 mm.

2.3 Experimental Procedure

This study investigates the relationship between the input parameters of the fused deposition modeling, a popular 3D printing technique, and the response factors to obtain the optimal combination of parameters. Printing

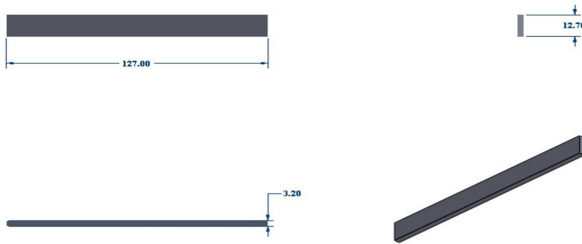


Figure 2: Flexural test specimen dimensions.

Table 2: Flexural Test Specimen Dimensions

Dimensions	Measurement in mm
Wo- Width Overall	12.7
l- Length Overall	125
T-Thickness	3.2

temperature, printing speed, layer thickness, number of contours, raster angle, and fill density were selected as the FDM process input parameter. Each factor and its working range were selected based on the literature review. Table 3 contains the input variables, their associated levels, and the response variables considered in this study.

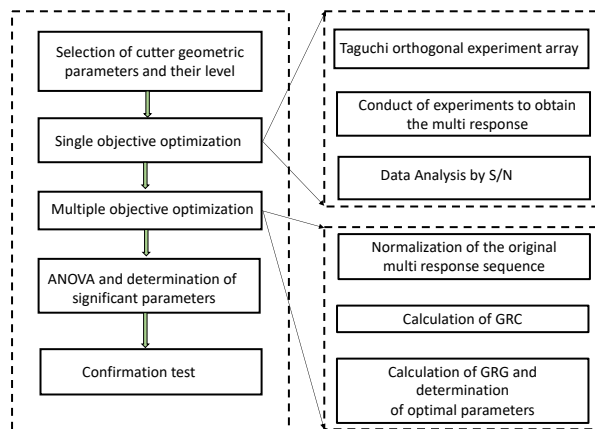


Figure 3: Flow Chart of Optimization steps.

The specimens were printed on Mankati Full-scale XT plus, keeping bed temperature, nozzle diameter, etc., constant. After printing the specimens, the test parts were

tested on a universal testing machine to determine the tensile and flexural strengths. Before the tensile and flexural tests, the specimens were measured using a digital Vernier slide caliper with a resolution of 0.02 mm to obtain the longitudinal shrinkage. Experiments were conducted in a random order as per the design matrix to eliminate systematic error. Finally, the Grey-Taguchi approach was used to determine the optimal parameters for the FDM process in terms of tensile strength, flexural strength, and longitudinal shrinkage. Figure 3 illustrates the flow chart of the optimization steps.

2.4 Design of Experiment

In this study, the Taguchi L27 orthogonal array (six factors three levels) was used as a statistical design of experiment (DOE) technique to assess how the FDM process behaves with the change in process input parameters selected. In this context, to construct the design matrix and analyze the test results, the statistical software Minitab version 17 was utilized. The factors considered for optimization were the printed parts' tensile strength, flexural strength, and longitudinal shrinkage. The multi-objective problem was then converted into a single-objective problem using Grey relational analysis, and the optimal FDM process parameters were determined. Additionally, the ANOVA test was used to quantify the contribution and influence of each input parameter on the FDM process's various responses. Table 5 illustrates the design matrix.

2.5 Measurement Method of Output Responses

2.5.1 Tensile Strength

In this study, tensile strength was measured using Shimadzu AGS-X. The parameters used for the test is given in Table 4.

2.5.2 Flexural Strength

During experimentation, the flexural strength was measured using the 3-point bending test using Shimadzu AGS-X. The loading nose and support used had a radius of 5 mm according to the specification given by ASTM-

Table 3: Control factors and their levels for PLA material.

Symbols	Input Factors	Units	Levels		
			1	2	3
A	Printing temperature	Celsius	230	235	240
B	Printing speed	mm/s	40	50	60
C	Layer thickness	mm	0.1	0.15	0.2
E	Number of contours	-	8	12	16
F	Raster angle	Degree	0	45	90
G	Fill density	Percentage	20	25	30
Response Factors	Tensile strength and Flexural strength				
Dimensional Accuracy	Longitudinal shrinkage				
Constant Factors	Bed temperature, Nozzle diameter, Material, build orientation, Air gap etc.				

Table 4: Tensile test machine parameters

Speed of testing (mm/min)	$5 \pm 25\%$
Nominal strain rate at start of test (mm/mm.min)	0.1

790-03. The parameters of the 3-point bending test are as follows:

During experimentation, the flexural strength was measured using the 3-point bending test using Shimadzu AGS-X. The loading nose and support used had a radius of 5 mm according to the specification given by ASTM-790-03. The parameters of the 3-point bending test are as follows:

Crosshead Motion,

$$R = \frac{ZL^2}{6d} = \frac{0.01 \times 51.2^2}{6 \times 3.2} = 1.3653 \text{ mm/min}$$

Where, R = rate of crosshead motion(mm/min), L = support span (mm), d = depth of beam(mm).

Z = rate of straining of the outer fiber(mm/mm/min). Z shall be equal to 0.01.

Flexural Stress,

$$\sigma_f = \frac{3PL}{2bd^2}$$

Where, σ_f = stress in the outer fibers at midpoint (MPa), P = load at the given point, on the load deflection curve(N), d = depth of beam(mm) and b = width of the beam (mm).

3 Process Optimization

3.1 Signal to Noise Analysis

Taguchi can be used in conjunction with Grey relational analysis (GRA) to optimize numerous performance attributes. In comparison to conventional results, Eqs. 1 and 2 can be used to find the smaller/higher and superior quality characteristics, respectively.

$$S/N \text{ ratio}(\eta) = -10 \log \left[\frac{1}{n} \sum_{i=1}^n Y_i^2 \right] \quad (1)$$

$$S/N \text{ ratio}(\eta) = -10 \log \left[\frac{1}{n} \sum_{i=1}^n \frac{1}{Y_i^2} \right] \quad (2)$$

Where Y_1, Y_2, \dots, Y_n are the individual responses for the trial condition, which occurs n times.

3.2 Optimization problem

The optimization problem that this study is attempting to solve can be stated as follows:

Minimize: Longitudinal Shrinkage

Maximize: Tensile strength, Flexural strength.

Subjected to:

$230 \leq \text{Temp.} \leq 240$; $40 \leq \text{Printing Speed} \leq 60$; $0.1 \leq \text{Layer Thickness} \leq 0.2$; $8 \leq \text{Number of Contours} \leq 16$; $0 \leq \text{Raster Angle} \leq 90$; $20 \leq \text{Fill Density} \leq 30$.

3.2.1 Grey-Taguchi multi-objective optimization method

Optimization challenges are generally classified as 'Maximization', 'Minimization', or 'Reach a target'. As the study includes the maximization of mechanical properties such as tensile strength and flexural strength and the minimization of longitudinal shrinkage, both the minimization and maximization categories were considered in this study.

3.2.2 Pre-processing of data

This stage converts the given data from various responses to a standard dimensionless scale of 0 to 1. This conversion is necessary as, in this case, each response has a unique scale. During conversion, the smaller, the better was used for longitudinal shrinkage, and the larger, the better was used for tensile and flexural strength. This idea was applied to all responses.

The longitudinal shrinkage is normalized to minimize the function by using Eq. 3

$$y_i(k) = \frac{\max x_i(k) - x_i(k)}{\max x_i(k) - \min x_i(k)} \quad (3)$$

The tensile strength and flexural strength are normalized to maximize the function by using Eq. 4

$$y_i(k) = \frac{x_i(k) - \min x_i(k)}{\max x_i(k) - \min x_i(k)} \quad (4)$$

Where k represents the responses and $x_i(k)$ is the sequence of longitudinal shrinkage, tensile strength, and flexural strength for an experimental run $i = 1 - 27$ prior to data preprocessing (i.e., original); $y_i(k)$ denotes longitudinal shrinkage, flexural strength, and tensile strength sequences for an experimental run $i = 1 - 27$ following data pre-processing; $\max x_i(k)$ is the highest value of actual data; $\min x_i(k)$ is the lowest value of the actual data [13].

3.2.3 Grey relational coefficient

After the original data have been pre-processed, the normalized data are utilized to estimate the grey relational

coefficient (GRC) values for all trials. The purpose of ascertaining the GRC is to establish a relationship between typical experimental values and normalized values.

In this study, Eq. 5 is used to calculate the GRC.

$$j_i(k) = \frac{\Delta_{\min} + C \cdot \Delta_{\max}}{\Delta_{0i}(k) + C \cdot \Delta_{\max}} \quad (5)$$

Here, the deviation sequence is denoted by Δ_{0i} . It is reported as an absolute value for the reference sequence $y_0(k)$ and comparability sequence $y_i(k)$. Thus, the Δ_{0i} , Δ_{\min} , and Δ_{\max} are estimated by the formulas shown in Eq 6-8. Although the differentiating coefficient has a value of $C \in [0, 1]$, this study used $C = 0.50$ [13].

The deviation sequence is given by:

$$\Delta_{0i}(k) = |y_0(k) - y_i(k)| \quad (6)$$

The minimum deviation is:

$$\min = \min_k \Delta_{0i}(k) \quad (7)$$

The maximum deviation is:

$$\Delta_{\max} = \max_k \Delta_{0i}(k) \quad (8)$$

3.2.4 Grey relational grade

When multiple outputs are considered, the GRC values were multiplied by the relevant weight value (0 to 1) of the output parameter. Then the products of GRC and weighted value are summed up for n number of testing to calculate the combined grey relational grade. Eq. 9 represents GRG.

$$\zeta(y_0, y_i) = \sum_{k=1}^n \omega_k J_k \quad (9)$$

Here, ω_k is the weight assigned to the k th input factor and the $\sum_{k=1}^n \omega_k = 1$.

Table 5: Design matrix with actual independent process variables.

Exp. No.	Printing Temp. (°C)	Print Speed (mm/s)	Layer Thickness (mm)	Num. of Contours	Raster Angle (°)	Fill Density (%)
1	230	40	0.1	8	0	20
2	230	40	0.1	8	45	25
3	230	40	0.1	8	90	30
4	230	50	0.15	12	0	20
5	230	50	0.15	12	45	25
6	230	50	0.15	12	90	30
7	230	60	0.2	16	0	20
8	230	60	0.2	16	45	25
9	230	60	0.2	16	90	30
10	235	40	0.15	16	0	25
11	235	40	0.15	16	45	30
12	235	40	0.15	16	90	20
13	235	50	0.2	8	0	25
14	235	50	0.2	8	45	30
15	235	50	0.2	8	90	20
16	235	60	0.1	12	0	25
17	235	60	0.1	12	45	30
18	235	60	0.1	12	90	20
19	240	40	0.2	12	0	30
20	240	40	0.2	12	45	20
20	240	40	0.2	12	45	20
21	240	40	0.2	12	90	25
22	240	50	0.1	16	0	30
23	240	50	0.1	16	45	20
24	240	50	0.1	16	90	25
25	240	60	0.15	8	0	30
26	240	60	0.15	8	45	20
27	240	60	0.15	8	90	25

4 Result and Discussions

4.1 Effect of Process Parameters on the Outputs

As mentioned earlier, a set of six parameters such as layer thickness, number of contours, printing temperature, printing speed, raster angle, and fill were considered in this study. The parametric effects of the factors mentioned above were established with the help of the point prediction method in Minitab software Version 17. In this section, the effects of process parameters will be shown and explained over output responses which are shown in Table 6 below.

4.1.1 Effect of Process Parameters on Tensile Strength

As shown in Table 7 and Fig. 4, data on signal-to-noise ratio were used to rank parameters and show their effects on the tensile strength of the specimen. From the table, it is evident that the layer thickness of the specimen while printing affects the tensile strength of the specimen the most.

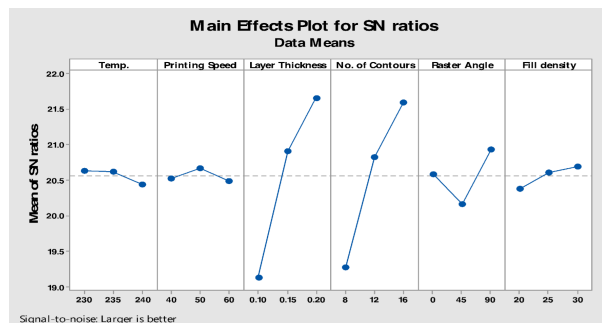


Figure 4: Main Effect Plot for SN Ratios for Tensile Strength.

Since the thicker the layer, the stronger the component, the tensile strength of the specimen increases noticeably with the layer thickness, as shown in Fig. 4. In the case of printing temperature, the highest tensile strength is found to achieve at 230°C. This is because of the efficient printing that depends on the closeness of the printing temperature to the material's melting point, which is around 230°C [14] in this study.

Table 6: Experimental Measured Responses

Exp. No.	Tensile strength (N/mm ²)	Flexural strength (MPa)	Longitudinal Shrinkage (%)
1	7.01599	25.1269	1.339
2	7.52256	25.8093	0.499
3	9.1190	35.3981	0.735
4	11.3968	40.6457	0.919
5	12.1734	32.9130	0.346
6	11.4591	37.4205	0.562
7	13.9445	44.3834	0.997
8	12.2350	46.3447	0.514
9	14.7705	47.5706	0.630
10	12.9845	42.8473	1.134
11	11.1276	39.4733	0.315
12	13.5449	38.0676	0.714
13	10.3771	36.5099	0.892
14	10.9607	37.9485	0.336
15	10.5346	32.9215	0.770
16	9.77630	28.1418	1.417
17	8.79410	37.2412	0.446
16	9.77630	28.1418	1.417
17	8.79410	37.2412	0.446
18	9.35381	31.2948	0.341
19	12.3491	42.2437	1.102
20	12.0700	34.2286	0.262
21	12.2350	41.0493	0.140
22	9.52574	36.7348	1.092
23	10.2592	31.2728	1.024
24	10.7300	35.5155	0.472
25	10.5487	31.7256	0.793
26	7.99327	31.2066	0.488
27	9.70939	34.8133	0.562

Besides, as the raster along the periphery of the layer increases with the number of contours, tensile strength increases with the contour's number. Again, when the specimen is printed at either 0 degrees or 90 degrees raster angle, the filaments remain parallel to the load direction, and hence, the specimen's tensile strength is higher at these raster angles. Any finite raster angle between the printed microstructural elements and load direction causes the filaments to be subjected to tensile stress and shear stress, leading to failure at low tensile strength. Similar results

Table 7: Signal to Noise ratio for tensile strength

Level	Print. Temp. (°C)	Print. Speed (mm/s)	Layer Thick. (mm)	Num. of Contours	Raster Angle (°)	Fill Density (%)
1	20.63	20.52	19.13	19.28	20.58	20.37
2	20.61	20.67	20.90	20.82	20.17	20.61
3	20.43	20.49	21.65	21.59	20.93	20.69
Delta	0.20	0.18	2.52	2.31	0.76	0.32
Rank	5	6	1	2	3	4

were found in [15]. The effect of fill density over the tensile strength of the specimen is relatively straightforward. The higher the specimen's density will have, the higher will be the specimen's tensile strength. Thus, tensile strength is found to increase with the increase of fill density.

Tensile strength increases with printing speed up to a specific limit and then decreases. Because with the rise in printing speed, the layer thickness increases, which plays a significant role in increasing the tensile strength of the specimen. However, if the printing speed crosses a certain level, then the specimen achieves a weaker interlayer bonding or interlayer porosity. As a result, a specimen's tensile strength decreases. Hence, the printing speed must be set at a level that is neither too high nor too low [16]. From Fig 4, it can be seen that the best tensile strength is found at the most moderate printing speed, which is around 50mm/s.

4.2 Effect of Process Parameters on Flexural Strength

The same six parameters show a similar effect on the flexural strength of the specimen. Nevertheless, there are some subtle differences. In the same way, as seen in Table 8, layer thickness plays a significant role in the flexibility of the specimen. With the increase of the layer thickness, the flexibility, and the ductility of the sample increases. It is shown in the signal to noise ratio graph that the specimen ends up with higher flexural stresses for the larger layer thickness with increasing the flexure extended by the specimen. The machine then acts.

The melting temperature range of the PLA for 3d printing is 195–215°C [17]. As the closest temperature to PLA's melting temperature is 230 degrees Celsius, the highest

flexural stress is achieved at this temperature [14]. Because the level of temperature is close to the melting temperature of PLA and, as a result, significantly less residual stress forms after cooling. As the printing speed increases, the interlayer bond gets weakened, resulting in higher ductility and lower brittleness, which ends up in a great deal of flexural strength. Moreover, with the de-

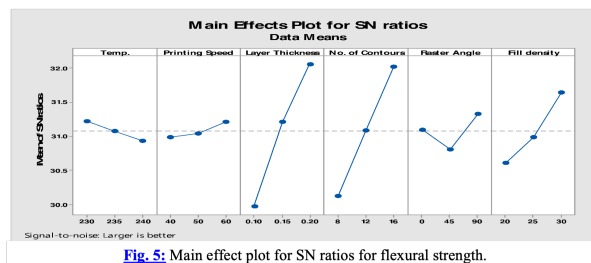


Fig. 5: Main effect plot for SN ratios for flexural strength.

Figure 5: Flexural test specimen dimensions.

crease in printing speed, the layer thickness decreases, and as a result, the flexibility decreases. So, the highest flexural strength can be achieved with an increase in printing speed. Now the number of contours plays their role in the flexural stress of the specimen, almost like the tensile strength as the raster angle the periphery layer will increase; it will increase the flexural strength of the specimen. So, the flexural strength increases with the number of contours. The raster angle of the specimen while printing plays the same role as it did on the tensile strength. From Fig. 5, it can be seen that the highest flexural strength can be achieved when the raster angle is 90 degrees.

Any other finite raster angle is obligated to shear stress and flexural strength, which causes a reduction in the flexural strength of the specimen. In the case of fill den-

Table 8: Signal to Noise ratio for flexural strength

Level	Print. temperature	Print. Speed	Layer Thickness	No. of Contours	Raster Angle	Fill Density
1	31.22	30.98	29.97	30.13	31.09	30.61
2	31.07	31.04	31.21	31.09	30.81	30.99
3	30.94	31.21	32.05	32.02	31.33	31.64
Delta	0.29	0.22	2.08	1.89	0.52	1.03
Rank	5	6	1	2	4	3

sity, the higher the fill density is, the greater ductility is achieved for the specimen resulting in higher flexural strength of the component.

4.3 Effect of process parameters on Longitudinal Shrinkage:

While the 3D printing parameters were directly affecting the tensile strength and the flexural strength of the specimen, longitudinal shrinkage cannot be determined entirely with the selected parameters as it largely depends on some other parameters like cooling system, bed, bed temperature, bed material, and how the specimen is unloaded from the bed. So, at the same six parameters, different levels of shrinkages can be found because of the bed temperature or cooling process, or even the bed material [18].

From Fig. 6 and Table 9, it can be seen that the most significant factor for the longitudinal shrinkage is the raster angle. Hence, it is better to print at 0° angle because the printing layer is on the longitudinal plane. The best temperature is 230°C for PLA because higher temperature causes thermal distortions as more longitudinal shrinkage happens seen from the research done by Coppola et al [14]. As the number of contours increases, the inter bond of the layer increases and consequently prevents the material from longitudinal shrinkage.

4.4 Process Parameter Optimization

4.4.1 Optimum Setting Process Parameters

The rank of the weighted grey relational grade is shown in Table 10; the highest GRG value, 0.85526, is designated as order 1, while the lowest GRG value, 0.3380, is labeled as order 27. According to works by Lin et al. [19] the greatest GRG value reflects the optimal system result,

i.e., in this work, experiment 9 represents the optimal factor level. Additionally, it indicates that printing at a temperature of 230°C , a speed of 60 mm/s, a layer thickness of 0.2 mm, a contour count of 16, a raster angle of 90° , and a fill density of 30% reveals the maximum tensile and flexural strength, as well as the minimum shrinkage. The response values for the optimal parameter levels are as follows: optimal tensile strength = 14.7705 N/mm², optimal flexural strength = 47.5706 MPa, and optimal longitudinal shrinkage = 0.630 percent of part's length (Table 6).

Table 10 indicates that experiment no-9 (Table 5) which entails level 1 of temperature (230°C), level 3 of printing speed (60 mm/s), level 3 of layer thickness (0.2 mm), level 3 of no. of contours (16), level 3 of raster angle (60°) and level 3 of fill density (30%) are the optimum factor levels for the combined tensile strength, flexural strength, and shrinkage. As shown in Table 10, the printing temperature is found the least important one among the factors considered in this study. Thus, Grey-Taguchi techniques' optimum combinations of input parameters are layer thickness-number of contours-raster angle-printing speed-fill density-printing temperature.

4.4.2 Analysis of Variance

Results of the ANOVA from Table 11 indicate that layer thickness is the most significant (43.70%) 3D printing factor affecting the multiple performance characteristics (tensile strength, flexural strength, and longitudinal shrinkage). After layer thickness, the second most significant factor is the number of contours with a contribution of 26.46%. Another parameter to mention is the raster angle with an 11.77% contribution for 3D printing parts concerning the tensile strength, flexural strength, and longitudinal shrinkage.

Table 9: Signal to Noise ratio for longitudinal shrinkage.

Level	Print. Temp. (°C)	Print. Speed (mm/s)	Layer Thick. (mm)	Num. of Cont.	Raster Angle (°)	Fill Dens. (%)
1	3.4393	5.1013	2.7842	3.5738	-0.4996	3.3805
2	4.2149	3.6938	4.4529	6.2396	7.2463	5.1682
3	5.1855	4.0447	5.6027	3.0265	6.0931	4.2911
Delta	1.7462	1.4075	2.8184	3.2131	7.7459	1.7877
Rank	5	6	3	2	1	4

Table 10: Grey relational coefficient and grey relational grade

Exp. No.	Tensile strength	Flexural Strength	Longitudinal Shrinkage	Grey Relation Grade	Rank
1	0.333333	0.333333	0.347483	0.338049887	27
2	0.348511	0.34023	0.6401	0.442947012	24
3	0.4069	0.479682	0.517633	0.468071841	21
4	0.534723	0.618394	0.450441	0.534519414	14
5	0.598864	0.43362	0.756069	0.596184186	9
6	0.539358	0.525073	0.602074	0.555501521	12
7	0.824377	0.778806	0.426948	0.676710013	4
8	0.604616	0.901519	0.630617	0.712250756	3
9	1	1	0.565795	0.855265101	1
10	0.684634	0.703779	0.391118	0.593176863	10
11	0.515582	0.580867	0.78488	0.627109771	6
12	0.759821	0.541469	0.526598	0.609295982	7
13	0.468797	0.503617	0.459187	0.47720031	18
14	0.504388	0.538373	0.765129	0.602629961	8
15	0.477897	0.433762	0.50335	0.471669879	20
16	0.437048	0.366122	0.333333	0.378834425	26
17	0.393484	0.520704	0.676019	0.530069114	15
18	0.417181	0.408102	0.760572	0.528618165	16
19	0.615569	0.678109	0.398938	0.564205263	11
20	0.58945	0.456844	0.839579	0.628624211	5
21	0.604616	0.63246	1	0.745691976	2
22	0.425044	0.50875	0.401446	0.445079958	23
23	0.462208	0.407775	0.419376	0.429786358	25
24	0.489691	0.4821	0.657908	0.54323331	13
25	0.478729	0.414598	0.494386	0.462571356	22

5 Conclusions

This study investigates the effect of process parameters on output responses and tries to optimize the process parameters in terms of tensile strength, flexural strength, and longitudinal shrinkage. Therefore, from the results and

discussion, the following conclusions can be drawn:

- The Grey-Taguchi approach is a precise strategy for optimizing FDM process parameters to create a printed object with the optimal tensile strength, flexural strength, and longitudinal shrinkage and determine the associated optimal set of FDM process pa-

Table 11: ANOVA result

Source	DF	Seq SS	Adj SS	Adj MS	F-Value	P-Value	Contribution
Temp. Printing Speed	2	0.00349	0.003489	0.00175	1.68	0.222	2.30%
Layer Thickness	2	0.06642	0.066424	0.03321	31.99	0	43.70%
No. of Contours	2	0.04022	0.040221	0.02011	19.37	0	26.46%
Raster Angle	2	0.01789	0.017893	0.00895	8.62	0.004	11.77%
Fill density	2	0.00473	0.004725	0.00236	2.28	0.139	3.11%
Error	14	0.01453	0.014534	0.00104	-	-	9.56%
Total	26	0.15199	-	-	-	-	100.00%

rameters.

- Layer thickness, number of contours, and the raster angle are the most significant parameters affecting tensile strength, flexural strength, and longitudinal shrinkage of the 3D printed parts.
- For this machine-material-process parameter combination, layer height, raster angle, fill density, the number of contours, printing temperature, and printing speed need to be set to 0.2 mm, 90 degrees, 30%, 16, 230°C and 60 mm/s respectively to minimize longitudinal shrinkage and maximize tensile and flexural strengths concurrently
- The results obtained from this study are expected to provide valuable information on improving the quality of the 3D printed object in terms of mechanical strength and dimensional accuracy. Moreover, these results help us maintain dimensional accuracy with tight tolerances, ensuring dimensional stability and repeatability of the manufactured part and enhancing the 3D printed product's durability and flexibility.

References

- [1] S. Coşkun, Y. Kayıkcı, and E. Gençay, "Adapting engineering education to industry 4.0 vision," *Technologies*, vol. 7, no. 1, p. 10, 2019.
- [2] "Astm international and iso unveil framework for global 3d printing standards," <https://sn.astm.org/outreach/astm-international-and-iso-unveil-framework-global-3d-printing-standards-nd16.html>, Year of Publication, accessed on 19 December 2023.
- [3] "Additive manufacturing 101," <https://www.thomasnet.com/insights/an-overview-of-additive-manufacturing/?cv=1>, 2021, retrieved 9 July 2021.
- [4] I. Gibson, D. W. Rosen, B. Stucker, M. Khorasani, D. Rosen, B. Stucker, and M. Khorasani, *Additive manufacturing technologies*. Springer, 2021, vol. 17.
- [5] L. K. Pan, C. C. Wang, S. L. Wei, and H. F. Sher, "Optimizing multiple quality characteristics via taguchi method-based grey analysis," *Journal of Materials Processing Technology*, vol. 182, no. 1-3, pp. 107–116, 2007.
- [6] M. Vaezi and C. K. Chua, "Effects of layer thickness and binder saturation level parameters on 3d printing process," *The International Journal of Advanced Manufacturing Technology*, vol. 53, pp. 275–284, 2011.
- [7] A. Lanzotti, M. Grasso, G. Staiano, and M. Martorelli, "The impact of process parameters on mechanical properties of parts fabricated in pla with an open-source 3-d printer," *Rapid Prototyping Journal*, vol. 21, no. 5, pp. 604–617, 2015.
- [8] S. K. Panda, S. Padhee, S. Anoop Kumar, S. S. Mahapatra *et al.*, "Optimization of fused deposition modelling (fdm) process parameters using bacterial foraging technique," *Intelligent information management*, vol. 1, no. 02, p. 89, 2009.

- [9] O. S. Es-Said, J. Foyos, R. Noorani, M. Mendelson, R. Marloth, and B. A. Pregger, "Effect of layer orientation on mechanical properties of rapid prototyped samples," *Materials and Manufacturing Processes*, vol. 15, no. 1, pp. 107–122, 2000.
- [10] S.-H. Ahn, M. Montero, D. Odell, S. Roundy, and P. K. Wright, "Anisotropic material properties of fused deposition modeling abs," *Rapid prototyping journal*, vol. 8, no. 4, pp. 248–257, 2002.
- [11] O. A. Mohamed, S. H. Masood, and J. L. Bhowmik, "Optimization of fused deposition modeling process parameters for dimensional accuracy using i-optimality criterion," *Measurement*, vol. 81, pp. 174–196, 2016.
- [12] D. C. Montgomery, *Design and analysis of experiments*. John wiley & sons, 2017.
- [13] P. Angappan, S. Thangiah, and S. Subbarayan, "Taguchi-based grey relational analysis for modeling and optimizing machining parameters through dry turning of incoloy 800h," *Journal of Mechanical Science and Technology*, vol. 31, pp. 4159–4165, 2017.
- [14] B. Coppola, N. Cappetti, L. Di Maio, P. Scarfato, and L. Incarnato, "3d printing of pla/clay nanocomposites: Influence of printing temperature on printed samples properties," *Materials*, vol. 11, no. 10, p. 1947, 2018.
- [15] W. Wu, P. Geng, G. Li, D. Zhao, H. Zhang, and J. Zhao, "Influence of layer thickness and raster angle on the mechanical properties of 3d-printed peek and a comparative mechanical study between peek and abs," *Materials*, vol. 8, no. 9, pp. 5834–5846, 2015.
- [16] J. Van Der Putten, G. De Schutter, and K. Van Tittelboom, "Surface modification as a technique to improve inter-layer bonding strength in 3d printed cementitious materials," *RILEM Technical Letters*, vol. 4, pp. 33–38, 2019.
- [17] D. J. Thomas and D. Singh, *3D Printing in Medicine and Surgery: Applications in Healthcare*. Woodhead Publishing, 2020.
- [18] C. Schmutzler, F. Bayerlein, S. Janson, C. Seidel, and M. F. Zaeh, "Pre-compensation of warpage for additive manufacturing," *Journal of Mechanics Engineering and Automation*, vol. 6, no. 8, pp. 392–399, 2016.
- [19] M.-Y. Lin, C.-c. Tsao, C.-y. Hsu, A.-h. Chiou, P.-c. Huang, and Y.-c. Lin, "Optimization of micro milling electrical discharge machining of inconel 718 by grey-taguchi method," *Transactions of Non-ferrous Metals Society of China*, vol. 23, no. 3, pp. 661–666, 2013.